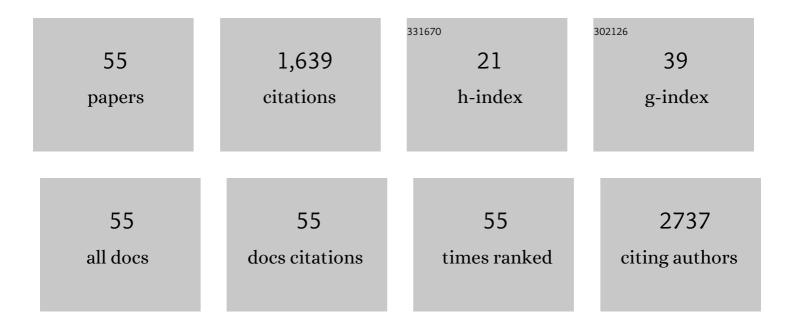
## Joel R Garbow

List of Publications by Year in descending order

Source: https://exaly.com/author-pdf/2708042/publications.pdf Version: 2024-02-01



#	Article	IF	CITATIONS
1	Estimation of the mechanical properties of a transversely isotropic material from shear wave fields via artificial neural networks. Journal of the Mechanical Behavior of Biomedical Materials, 2022, 126, 105046.	3.1	7
2	Editorial on "Ex vivo <scp>MRI</scp> of the Normal Human Placenta: Structuralâ€Functional Interplay and the Association With Birth Weight― Journal of Magnetic Resonance Imaging, 2022, 56, 145-146.	3.4	0
3	Multiâ€band echoâ€planar spectroscopic imaging of hyperpolarized <sup>13</sup> C probes in a compact preclinical PET/MR scanner. Magnetic Resonance in Medicine, 2022, 87, 2120-2129.	3.0	1
4	Comparison of hyperpolarized <sup>13</sup> C and nonâ€hyperpolarized deuterium MRI approaches for imaging cerebral glucose metabolism at 4.7 T. Magnetic Resonance in Medicine, 2021, 85, 1795-1804.	3.0	20
5	<sup>15</sup> Nâ€carnitine, a novel endogenous hyperpolarized MRI probe with long signal lifetime. Magnetic Resonance in Medicine, 2021, 85, 1814-1820.	3.0	11
6	Dynamic Contrast Enhancement (DCE) MRI–Derived Renal Perfusion and Filtration: Basic Concepts. Methods in Molecular Biology, 2021, 2216, 205-227.	0.9	3
7	Analysis Protocol for Dynamic Contrast Enhanced (DCE) MRI of Renal Perfusion and Filtration. Methods in Molecular Biology, 2021, 2216, 637-653.	0.9	1
8	Irradiation-Modulated Murine Brain Microenvironment Enhances GL261-Tumor Growth and Inhibits Anti-PD-L1 Immunotherapy. Frontiers in Oncology, 2021, 11, 693146.	2.8	5
9	Metabolite-Specific Echo-Planar Imaging of Hyperpolarized [1-13C]Pyruvate at 4.7 T. Tomography, 2021, 7, 466-476.	1.8	2
10	Strain differences in the extent of brain injury in mice after tetramethylenedisulfotetramine-induced status epilepticus. NeuroToxicology, 2021, 87, 43-50.	3.0	1
11	A MYT1L syndrome mouse model recapitulates patient phenotypes and reveals altered brain development due to disrupted neuronal maturation. Neuron, 2021, 109, 3775-3792.e14.	8.1	34
12	Asthma reduces glioma formation by T cell decorin-mediated inhibition of microglia. Nature Communications, 2021, 12, 7122.	12.8	21
13	Alteration of Cellular Reduction Potential Will Change 64Cu-ATSM Signal With or Without Hypoxia. Journal of Nuclear Medicine, 2020, 61, 427-432.	5.0	11
14	Radiolabeled 6-(2, 3-Dichlorophenyl)-N4-methylpyrimidine-2, 4-diamine (TH287): A Potential Radiotracer for Measuring and Imaging MTH1. International Journal of Molecular Sciences, 2020, 21, 8860.	4.1	3
15	Comparative Uptake and Biological Distribution of [18F]-Labeled C6 and C8 Perfluorinated Alkyl Substances in Pregnant Mice via Different Routes of Administration. Environmental Science and Technology Letters, 2020, 7, 665-671.	8.7	10
16	Estimation of Anisotropic Material Properties of Soft Tissue by MRI of Ultrasound-Induced Shear Waves. Journal of Biomechanical Engineering, 2020, 142, .	1.3	13
17	Connexin43 Expression and Associated Chronic Inflammation Presages the Development of Cerebral Radiation Necrosis. Journal of Neuropathology and Experimental Neurology, 2020, 79, 791-799.	1.7	0
18	Longitudinal preclinical magnetic resonance imaging of diffuse tumor burden in intramedullary myeloma following bortezomib therapy. NMR in Biomedicine, 2019, 32, e4122.	2.8	0

JOEL R GARBOW

#	Article	IF	CITATIONS
19	Late Effects of Radiation Prime the Brain Microenvironment for Accelerated Tumor Growth. International Journal of Radiation Oncology Biology Physics, 2019, 103, 190-194.	0.8	25
20	Effects of an artificial placenta on brain development and injury in premature lambs. Journal of Pediatric Surgery, 2018, 53, 1234-1239.	1.6	22
21	Bayesian Modeling of NMR Data: Quantifying Longitudinal Relaxation in Vivo, and in Vitro with a Tissue-Water-Relaxation Mimic (Crosslinked Bovine Serum Albumin). Applied Magnetic Resonance, 2018, 49, 3-24.	1.2	4
22	Inhibitors of HIF-1α and CXCR4 Mitigate the Development of Radiation Necrosis in Mouse Brain. International Journal of Radiation Oncology Biology Physics, 2018, 100, 1016-1025.	0.8	25
23	Preclinical MRI: Studies of the irradiated brain. Journal of Magnetic Resonance, 2018, 292, 73-81.	2.1	1
24	Modeling Dynamic Contrast-Enhanced MRI Data with a Constrained Local AIF. Molecular Imaging and Biology, 2018, 20, 150-159.	2.6	5
25	Intracellular water preexchange lifetime in neurons and astrocytes. Magnetic Resonance in Medicine, 2018, 79, 1616-1627.	3.0	51
26	A magnetic resonance imaging study of early brain injury in a rat model of acute DFP intoxication. NeuroToxicology, 2018, 66, 170-178.	3.0	25
27	Assessing Mucosal Inflammation in a DSS-Induced Colitis Mouse Model by MR Colonography. Tomography, 2018, 4, 4-13.	1.8	16
28	IMMU-05. LATE EFFECTS OF INTRACRANIAL RADIATION INDUCES RESISTANCE TO IMMUNE CHECKPOINT BLOCKADE THERAPY THAT IS PARTIALLY REVERSIBLE WITH CSF-1R INHIBITION. Neuro-Oncology, 2018, 20, vi122-vi122.	1.2	0
29	Discriminating radiation injury from recurrent tumor with [18F]PARPi and amino acid PET in mouse models. EJNMMI Research, 2018, 8, 59.	2.5	16
30	Minoxidil improves vascular compliance, restores cerebral blood flow, and alters extracellular matrix gene expression in a model of chronic vascular stiffness. American Journal of Physiology - Heart and Circulatory Physiology, 2018, 315, H18-H32.	3.2	44
31	OSM potentiates preintravasation events, increases CTC counts, and promotes breast cancer metastasis to the lung. Breast Cancer Research, 2018, 20, 53.	5.0	38
32	Are complex DCEâ€MRI models supported by clinical data?. Magnetic Resonance in Medicine, 2017, 77, 1329-1339.	3.0	40
33	Can anti-vascular endothelial growth factor antibody reverse radiation necrosis? A preclinical investigation. Journal of Neuro-Oncology, 2017, 133, 9-16.	2.9	16
34	Perfluorocarbon emulsions radiosensitise brain tumors in carbogen breathing mice with orthotopic GL261 gliomas. PLoS ONE, 2017, 12, e0184250.	2.5	16
35	O <sub>2</sub> â€sensitive MRI distinguishes brain tumor versus radiation necrosis in murine models. Magnetic Resonance in Medicine, 2016, 75, 2442-2447.	3.0	43
36	MR Imaging–derived Oxygen-Hemoglobin Dissociation Curves and Fetal-Placental Oxygen-Hemoglobin Affinities. Radiology, 2016, 280, 68-77.	7.3	24

JOEL R GARBOW

#	Article	IF	CITATIONS
37	A complement–microglial axis drives synapse loss during virus-induced memory impairment. Nature, 2016, 534, 538-543.	27.8	534
38	O2-sensitive MRI distinguishes brain tumor versus radiation necrosis in murine models. Magnetic Resonance in Medicine, 2016, 75, spcone-spcone.	3.0	0
39	A Gamma-Knife-Enabled Mouse Model of Cerebral Single-Hemisphere Delayed Radiation Necrosis. PLoS ONE, 2015, 10, e0139596.	2.5	31
40	Specificity of vascular endothelial growth factor treatment for radiation necrosis. Radiotherapy and Oncology, 2015, 117, 382-385.	0.6	14
41	Perilesional edema in radiation necrosis reflects axonal degeneration. Radiation Oncology, 2015, 10, 33.	2.7	12
42	Estimation of material parameters from slow and fast shear waves in an incompressible, transversely isotropic material. Journal of Biomechanics, 2015, 48, 4002-4009.	2.1	46
43	Anti-VEGF Antibodies Mitigate the Development of Radiation Necrosis in Mouse Brain. Clinical Cancer Research, 2014, 20, 2695-2702.	7.0	64
44	Toward Distinguishing Recurrent Tumor From Radiation Necrosis: DWI and MTC in a Gamma Knife–Irradiated Mouse Glioma Model. International Journal of Radiation Oncology Biology Physics, 2014, 90, 446-453.	0.8	27
45	A CSK-3Î <sup>2</sup> Inhibitor Protects Against Radiation Necrosis in Mouse Brain. International Journal of Radiation Oncology Biology Physics, 2014, 89, 714-721.	0.8	20
46	Magnetic Resonance Imaging Defines Cervicovaginal Anatomy, Cancer, and VEGF Trap Antiangiogenic Efficacy in Estrogen-Treated K14-HPV16 Transgenic Mice. Cancer Research, 2009, 69, 7945-7952.	0.9	8
47	Diffusion-weighted and dynamic contrast-enhanced imaging as markers of clinical behavior in children with optic pathway glioma. Pediatric Radiology, 2008, 38, 1293-1299.	2.0	49
48	Actively decoupled transmit–receive coilâ€pair for mouse brain MRI. Concepts in Magnetic Resonance Part B, 2008, 33B, 252-259.	0.7	19
49	Quantitative Monitoring of Adenocarcinoma Development in Rodents by Magnetic Resonance Imaging. Clinical Cancer Research, 2008, 14, 1363-1367.	7.0	30
50	Exponential model selection (in NMR) using Bayesian probability theory. Concepts in Magnetic Resonance Part A: Bridging Education and Research, 2005, 27A, 64-72.	0.5	26
51	Exponential parameter estimation (in NMR) using Bayesian probability theory. Concepts in Magnetic Resonance Part A: Bridging Education and Research, 2005, 27A, 55-63.	0.5	60
52	Detection of Primary Lung Tumors in Rodents by Magnetic Resonance Imaging. Cancer Research, 2004, 64, 2740-2742.	0.9	49
53	A simple, robust hardware device for passive or active respiratory gating in MRI and MRS experiments. Concepts in Magnetic Resonance, 2004, 21B, 40-48.	1.3	26
54	Hyperpolarized3He MRI of mouse lung. Magnetic Resonance in Medicine, 2004, 52, 1310-1317.	3.0	64

#	Article	IF	CITATIONS
55	Synthesis and Characterization of a Gd-DOTA- <scp>D</scp> -Permeation Peptide for Magnetic Resonance Relaxation Enhancement of Intracellular Targets. Molecular Imaging, 2003, 2, 153535002003031.	1.4	6